j Dependence of the (^{19}F, ^{16}O) Reaction and Spin-Orbit Forces in the Heavy-Ion Optical Potential*

S. Kubono, D. Dehnhard, D. A. Lewis, T. K. Li, J. L. Artz, D. J. Weber, P. J. Ellis, and A. Dudek-Ellis
School of Physics and Astronomy, University of Minnesota, Minneapolis, Minnesota 55455
(Received 14 February 1977)

The shapes of the observed angular distributions for the reactions ^{28,30}Si(^{19}F, ^{16}O)^{31,33}P to $\frac{3}{2}^+$ and $\frac{5}{2}^+$ states differ strongly. A consistent description of this j dependence and of the ground-state $\frac{1}{2}^+$ angular distributions is given by distorted-wave Born-approximation calculations which assume triton cluster transfer and include spin-orbit potentials in both entrance and exit channels. We find from coupled-channel Born-approximation calculations that inelastic excitation of ^{19}F does not affect the shapes significantly.

Rather little is known about spin-dependent terms in the heavy-ion optical potential, although recent work[1] with a polarized ^{6}Li beam has shown the need for a spin-orbit $\vec{l}\cdot\vec{s}$ term. Transfer reactions in principle should be sensitive to spin-dependent forces. However, when using heavy ions, one is concerned with the transfer of a particle from an (l_2, j_2) orbital in the projectile to an (l_1, j_1) orbital in the residual nucleus. The angular momentum selection rules for a one-step process usually then allow several values of the transferred angular momentum L, and these can differ according to whether the angular momentum transferred to the target nucleus, j_1, is $l_1 + \frac{1}{2}$ or $l_1 - \frac{1}{2}$. This difference in L gives rise to a strong j_1 dependence even in the absence of spin-dependent potentials.[2] In the present work we choose a case where $l_2 = 0$ so that $L = l_1$ uniquely and the dependence of the angular distribution on j_1 for a given L can be observed.

Specifically we have studied the reactions ^{28,30}Si(^{19}F, ^{16}O)^{31,33}P at $E_{lab} = 60$ MeV. We assume that these reactions transfer a tritonlike cluster of three particles in a relative 0s state, thereby preserving the simplicity of a one-particle transfer process. This assumption should be well justified for the $\langle ^{16}\mathrm{O}|^{19}\mathrm{F}\rangle$ overlap since 92% of the ^{19}F wave function can be expressed[3,4] in terms of a cluster moving with angular momentum $l_2 = 0$ with respect to the ^{16}O core. The $\langle \mathrm{Si}|\mathrm{P}\rangle$ overlap presumably involves a number of components, however the relative 0s cluster should dominate the reaction since (1) this allows the c.m. wave function to extend as far out as possible which is important for surface reactions and (2) this does not require rearrangement of the three particles during the transfer process. Since $l_2 = 0$ with the cluster assumption, we have, as remarked, $L = l_1$ uniquely. Furthermore, since the target spin is zero, the spin of the residual nucleus is j_1. Thus we can compare $L = 2$ transfer to the lowest $\frac{3}{2}^+$ and $\frac{5}{2}^+$ states of ^{31}P and ^{33}P; we also study $L = 0$ transfer to the $\frac{1}{2}^+$ ground states.

The experiments were carried out with a 60-MeV ^{19}F^{6+} beam from the MP tandem van de Graaff accelerator of the University of Minnesota using a sputter-type ion source and Freon as source gas. Beam currents of 300–500 nA of ^{19}F(6^+) were used to bombard isotopically enriched SiO_2 targets (about 50 μg/cm^2), which had a carbon backing (about 5 μg/cm^2). The targets were continuously rotated while in the beam to reduce target deterioration. The reaction products were momentum analyzed by an Enge split-pole magnetic spectrograph. Three charge states ($6^+, 7^+, 8^+$) of ^{16}O, which include more than 99% of all ^{16}O ions in the present experiment, were detected simultaneously by position-sensitive, solid-state detectors placed along the focal surface. The spectrograph entrance aperture was set to 0.568 msr corresponding to an angular acceptance of 1°. We have also measured the ^{19}F elastic scattering on ^{28,30}Si at $E_{lab} = 60$ MeV between $\theta_{c.m.} = 10°$ and 60°. The optical-potential parameters deduced from these data are given in Table I as sets I and II for ^{28}Si and set III for ^{30}Si.

The experimental angular distributions for the transitions to the lowest $\frac{1}{2}^+$, $\frac{3}{2}^+$, and $\frac{5}{2}^+$ states of ^{31}P and ^{33}P are shown in Fig. 1. Note the dramatic difference in the observed angular distributions for the $\frac{3}{2}^+$ and $\frac{5}{2}^+$ states which both correspond to $L = 2$ transfer. This is strikingly similar to the j_1 dependence observed in (α, p) reactions,[5,6] as we discuss further below.

We have carried out finite-range full-recoil distorted-wave Born-approximation (DWBA) calculations, with the code[7] LOLA, in the post represen-

TABLE I. Optical-potential parameters.

Channel		V (MeV)	r_r (fm)	a_r (fm)	W (MeV)	r_I (fm)	a_I (fm)	V_{ls} (MeV)	r_{ls} (fm)	a_{ls} (fm)	r_c (fm)
$^{19}F+^{28}Si$	Set I	25.5	1.29	0.56	48.1	1.06	0.67				1.20
$^{19}F+^{28}Si$	Set II	28.9	1.39	0.44	16.3	1.02	0.80	3.0	1.35	0.40	1.20
$^{19}F+^{28}Si$	Set II′	30.5	1.36	0.46	8.1	1.21	0.72	3.0	1.35	0.40	1.20
$^{19}F+^{30}Si$	Set III	24.6	1.27	0.63	49.0	1.15	0.64				1.20
$^{16}O+^{31}P$	Set IV	23.6	1.35	0.47	12.6	1.27	0.26				1.35
$^{16}O+^{31}P$	Set V	31.2	1.45	0.47	15.1	1.27	0.31	0.75	1.24	0.37	1.35
Note a		Note b	1.25	0.65				6.3	1.25	0.65	1.25

[a] Triton bound state (see text).
[b] Adjusted to fit separation energy.

tation. In these calculations, potential sets I or III of Table I were employed in the entrance channel, and set IV in the exit channel. The latter was taken from an analysis[8] of ^{16}O scattering on ^{32}S since no elastic data exist for $^{16}O+^{31}P$. As regards triton bound-state parameters rather little is known, so we simply adopted the usual proton values except that the radius parameter was increased a little by using the prescription $r(A_{\text{core}}+3)^{1/3}$ on the basis of the α particle work of Arima and Yoshida.[9]

The DWBA results given by the full curves in Fig. 1 are completely out of phase with the data for the $\frac{1}{2}^+$ and $\frac{3}{2}^+$ levels; such anomalies have been found previously in some single-nucleon-transfer reactions, e.g., Bond *et al.*[10] Furthermore, the striking difference in the shapes of the

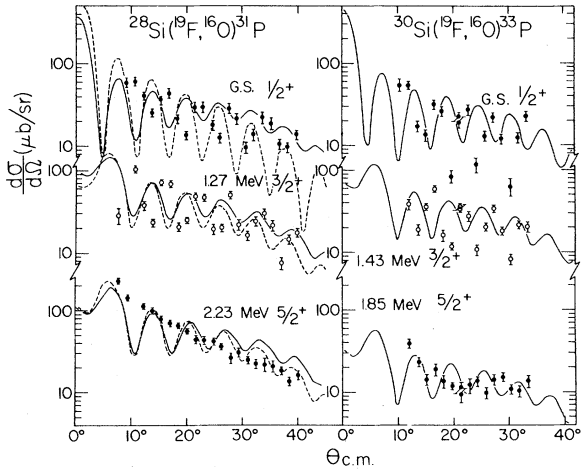

FIG. 1. Angular distributions of the reactions $^{28,30}Si(^{19}F,^{16}O)$ at $E_{lab}=60$ MeV leading to the lowest $\frac{1}{2}^+$, $\frac{3}{2}^+$, and $\frac{5}{2}^+$ levels of $^{31,33}P$. The full and dashed lines are, respectively, the result of the DWBA and CCBA calculations without spin-orbit forces which are discussed in the text.

$\frac{3}{2}^+$ and $\frac{5}{2}^+$ angular distributions is not reproduced by DWBA calculations. As is to be expected, the difference in binding energies for the two states and the assumed bound state $\vec{l}\cdot\vec{s}$ potential were found to produce only a minor j_1 dependence. It is worth remarking that in the case of transfer of an excited triton with $l_2=1$ with respect to the ^{16}O core, the angular distributions for the $\frac{1}{2}^+$ and $\frac{3}{2}^+$ levels have the correct phasing. However, the magnitude of the cross sections is estimated to be at least a factor of 100 smaller than obtained above.

The cross sections in Fig. 1, obtained with LOLA, have been normalized to the data; if the absolute cross section for the $\frac{1}{2}^+$ level is compared to the data a product of spectroscopic factors $\theta_1^2\theta_2^2=0.45$ is found. This is rather large since the shell model[3,4] gives $\theta_2^2=0.32$ for the projectile system and one would expect a significantly smaller value for the residual nucleus system. (Values of $\theta_1^2\theta_2^2=0.36$ and 0.16 are needed for the $\frac{3}{2}^+$ and $\frac{5}{2}^+$ levels, respectively.) We note that the magnitudes are found to be sensitive to the optical parameters and further that such discrepancies often arise in multinucleon transfers. We shall focus in the following on the shapes of the angular distributions. For this purpose it is sufficient to use the no-recoil approximation, since we have found that it gives results which differ from the full-recoil case mainly in magnitude, with only a small change in phase at the largest angles of interest here.

We first consider the effects of multistep processes since, for example, this improves the phasing[11] in the reaction $^{19}F(^{16}O,\,^{15}N)^{20}Ne$. It is most natural to study inelastic excitations of ^{19}F since this nucleus is known to be strongly deformed. Accordingly we have carried out a coupled-channel Born-approximation (CCBA)

calculation allowing inelastic excitation of the 0.197-MeV, $\frac{5}{2}^+$ and 1.56-MeV, $\frac{3}{2}^+$ levels of ^{19}F. Deformation parameters[12] $\beta_2 = 0.4$ and $\beta_4 = 0.14$ were used for the inelastic excitation and the optical-potential set I of Table I was used without adjustment since the fit to the elastic data was little affected. The relative spectroscopic amplitudes of Ref. 3 were used, and care was taken to ensure a consistent choice of phases. The transfer from factors were generated[13] in the no-recoil approximation using the bound-state parameters of Table I. The resulting CCBA predictions, normalized to the data, are given by the dashed curves in Fig. 1 and it is seen that they are qualitatively quite similar to the original DWBA results.

Now as we have remarked, the difference between the observed $\frac{3}{2}^+$ and $\frac{5}{2}^+$ angular distributions is reminiscent of earlier ^{28}Si$(\alpha,p)^{31}$P work.[5,6] Although for this particular target the effect is strongly energy dependent,[14] the general tendency observed in a number of (α,p) reactions[5,6,14,15] is for $j_1 = l_1 + \frac{1}{2}$ angular distributions to be less structured than those for $j_1 = l_1 - \frac{1}{2}$. This can be explained within the DWBA by spin-orbit effects. Accordingly for the present reaction that we have studied the effect of including spin-orbit potentials of the standard form, except that $\vec{l}\cdot\vec{s}$ is replaced by $(\vec{l}\cdot\vec{s} + \vec{I}\cdot\vec{I})$ where $\vec{s}$ is the spin of the projectile or ejectile and $\vec{I}$ is the spin of the target or residual nucleus. In our case the $\vec{l}\cdot\vec{s}$ term acts in the entrance channel and the $\vec{I}\cdot\vec{I}$ term in the exit channel. We have obtained potential set II (Table I) for the entrance channel which includes a spin-orbit interaction and which fits the elastic data. For the exit channel there is no elastic data, but we have obtained set V of Table I under the constraint that it gives roughly the same elastic angular distribution as the spin-independent set IV, i.e., about the same falloff with angle and similar oscillations beyond 45°. Now by using sets II and V in a no-recoil DWBA calculation and normalizing to the data, the full curves of Fig. 2 were obtained. These now show substantial agreement with the data, both as regards the j_1 dependence and the phasing.

Before systematically searching on the optical parameters, we plan to take elastic data for ^{16}O $+ ^{31}$P. A few comments should be made, however, on the parameters chosen. Firstly, we have exploited the sensitivity of the results to the real depth and the various radii of the exit-channel optical potential, while constraining the elastic angular distribution as discussed above. Secondly we have examined various spin-orbit strengths. The best results were obtained with a fairly large value in the entrance channel [which gives a strong absorption radius of 8.9 (9.8) fm for spin down (up)] and a smaller value in the exit channel. Thus some degree of "mismatch" seems necessary.

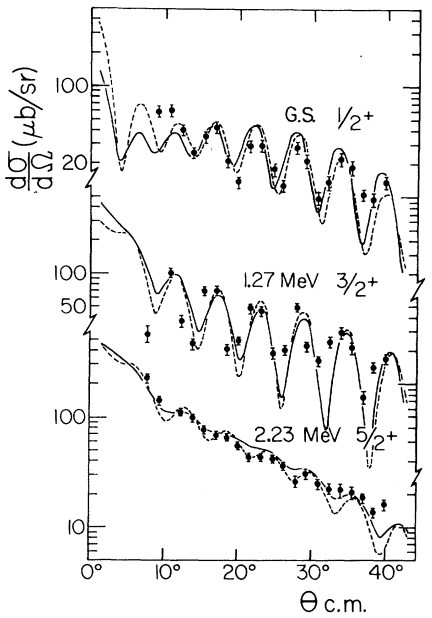

FIG. 2. Comparison of the observed angular distributions for the reaction ^{28}Si(^{19}F, ^{16}O)^{31}P with DWBA (full curve) and CCBA (dashed curve) calculations with spin-orbit forces (see text).

Finally, we carried out CCBA calculations as before, but with the spin-dependent optical potentials II′ and V of Table I. The former is an adjusted version of II which retains a fit to the elastic data. The CCBA results, normalized[16] to the data, are given by the dashed curves in Fig. 2. The multistep processes do not greatly affect the shapes, although an improvement is noted, particularly for the $\frac{5}{2}^+$ state.

We conclude that multistep processes, at least those involving inelastic excitation of ^{19}F, are unable to account for the observed data in the reaction ^{28}Si(^{19}F, ^{16}O)^{31}P. However, both the j_1 dependence and the phasing of the experimental angular distributions can be accounted for by including spin-orbit terms in both the entrance and exit channels. Clearly further work is needed to determine whether this is the correct physical interpretation. It is, however, supported by the similarity to previous (α,p) work.

We thank B. F. Bayman for helpful discussions.

*Work supported in part by the U. S. Energy Research and Development Administration Contracts No. E(11-1)-1265 and No. AT(11-1)1764; this is Report No. COO-1265-184.

[1]W. Weiss *et al.*, Phys. Lett. 61B, 237 (1976).
[2]W. Henning, D. G. Kovar, J. R. Erskine, and L. R. Greenwood, Phys. Lett. 55B, 49 (1975).
[3]P. J. Ellis and T. Engeland, Nucl. Phys. A144, 161 (1970).
[4]N. Anyas-Weiss *et al.*, Phys. Rep. 12C, 201 (1974).
[5]T. Yamazaki, M. Kondo, and S. Yamabe, J. Phys. Soc. Jpn. 18, 620 (1963).
[6]L. L. Lee *et al.*, Phys. Rev. Lett. 14, 261 (1965).
[7]R. M. DeVries, private communication.
[8]D. Dehnhard *et al.*, Phys. Rev. C 13, 164 (1976).
[9]A. Arima and S. Yoshida, Nucl. Phys. A219, 475 (1974).
[10]P. D. Bond *et al.*, Phys. Rev. Lett. 36, 300 (1976).
[11]K. S. Low, T. Tamura, and T. Udagawa, Phys. Rev. C 12, 3579 (1976).
[12]R. de Swiniarski *et al.*, Phys. Lett. 43B, 27 (1973); T. P. Krick, N. M. Hintz, and D. Dehnhard, Nucl. Phys. A216, 549 (1973).
[13]B. F. Bayman, unpublished.
[14]L. S. August, P. Shapiro, L. R. Cooper, and C. D. Bond, Phys. Rev. C 4, 2291 (1971).
[15]R. O. Ginaven and A. M. Bernstein, Nucl. Phys. A154, 417 (1970).
[16]Using unit spectroscopic factors for the $\langle^{28}\mathrm{Si}|^{31}\mathrm{P}\rangle$ overlaps and theoretical values for the $\langle^{16}\mathrm{O}|^{19}\mathrm{F}\rangle$ overlaps, the predicted CCBA $\frac{1}{2}^+$, $\frac{3}{2}^+$, and $\frac{5}{2}^+$ angular distributions have been multiplied, respectively, by normalization factors of 0.19, 0.23, and 0.044 to obtain the results of Fig. 2. The corresponding DWBA normalization factors are 0.17, 0.18, and 0.027. In both cases, the no-recoil approximation was used and spin-orbit forces were included. The relative magnitude of the normalization factors for the $\frac{3}{2}^+$ and $\frac{5}{2}^+$ states quoted here differs from that obtained in the LOLA (full-recoil) calculations without spin-orbit forces.

Vibrational Excitation of Polar Molecules by Slow Electrons: HCl†

L. Dubé and A. Herzenberg
Department of Engineering and Applied Science, Yale University, New Haven, Connecticut 06520
(Received 22 November 1976)

Shape resonances cannot explain the strong vibrational excitation observed in the impact of electrons on polar molecules at threshold, because an important s-wave component in the wave function inhibits trapping. We explain the main features observed in HCl by invoking the concept of a virtual state to account for an enhancement of the wave function of a slow departing electron.

Very large cross sections ($\sim 10^{-15}$ cm^2) have recently been observed for electrons exciting vibrations in polar molecules near the lowest vibrational threshold.[1,2] Within 0.5 eV of the thresholds, the observed cross sections are larger by factors of 10–100 than estimates with Born's approximation.[3]

Up to now, the dominant mechanism for vibrational excitation of molecules by electron impact at energies below 10 eV has been thought to be temporary trapping of the incoming electron in a compound state at a shape resonance.[4] However, the shape resonance mechanism cannot explain the large vibrational excitation cross sections observed at thresholds[1,2] because in this case there can be no trapping within a centrifugal potential barrier, as at an electron shape resonance in a molecule. Such trapping is impossible because the angular distributions suggest a strong s wave,[1,2] through which an electron can escape without having to tunnel through a centrifugal barrier.

In HCl, the total cross section near the threshold for the excitation $v=0\rightarrow v=1$ (where v is the vibrational quantum number) shows a peak about 0.2 eV wide[1]; at the peak, the cross section (integrated over scattering angles) reaches 2×10^{-15} cm^2 (see Fig. 1). At the next threshold, there is a similar but smaller peak for $v=0\rightarrow v=2$, but none for $v=0\rightarrow v=1$.

We have considered how the threshold peaks might arise from an enhancement of the wave funtion of a very slow departing electron at the molecule. Consider first a fictitious molecule which is roughly spherically symmetric, and whose potential vanishes outside a radius r_0 of molecular dimensions. Let the final state $\psi_f(r,k)$ be an s wave, normalized so that its incoming part as $r\rightarrow\infty$ is $(-)\exp[-i(kr+\delta_f)]/(2ikr)$, where r is the distance of the electron from the mass center, k is the wave number, and δ_f is the phase shift. ψ_f is defined for an electron in the potential from a molecule with nuclei frozen at their equilibrium positions. One finds $\psi_f(r_0,k=0)=1-a/r_0$, where a is the scattering length.[5] The corresponding amplitude for the free incident wave is 1, so that strong enhancement of the amplitude [i.e., $|\psi_f(r_0,$